Journal of Biomedical & Pharmaceutical Engineering 2:1 (2008) 29-35
ISSN: 1793-4532

Thermo-Responsive Hydrogel-Coated Gold Nanoshells for *In Vivo* Drug Delivery

Jun-Hyun Kim and T. Randall Lee*

Department of Chemistry, University of Houston, Houston, TX, USA

Corresponding Author: T. Randall Lee; Mailing Address: 4800 Calhoun Road, Houston, TX 77004-5003; Tel: 713-743-2724; Fax: 281-754-4445; Email: trlee@uh.edu

Abstract

This paper describes the preparation and characterization of a new type of composite nanoparticle, where the structure consists of a nontoxic hydrogel polymer network that encapsulates a gold shell/silica core. These composite nanoparticles are being developed as photothermally responsive drug-delivery vehicles that undergo structural changes slightly above physiological temperature. A unique property of these nanoparticles is that the hydrogel coatings can be collapsed by exposure to light via excitation of the strong plasmon resonance of the gold shell/silica core; this excitation provides a ready source of heat to the system. Furthermore, the gold nanoshell (GNS) cores were designed to absorb light at near-infrared wavelengths (800–1200 nm), which can pass readily through tissue and water. The thermo-responsive hydrogel coatings were prepared by free radical polymerization of a selected mixture of N-isoproprylacrylamide (NIPAM) and acrylic acid (AAc) in the presence of the GNS core particles. The resultant composite particles were characterized structurally and compositionally by FE-SEM, TEM, and EDX, respectively. UV-vis spectroscopy was used to characterize the optical properties, and DLS was used to determine the average diameter as a function of temperature. As a whole, the results presented here demonstrate that these composite nanoparticles can be reliably prepared and characterized; moreover, their systematic responses to variations in temperature are consistent with their intended use as discrete nanoscale drug-delivery vehicles.

Keywords: hydrogel, gold nanoshell, thermo-responsive, drug delivery, N-isopropylacrylamide, acrylic acid

Received 12 January 2007; revised and accepted 3 February 2007

1 INTRODUCTION

Substantial effort has focused on the preparation and study of nanostructured materials (e.g., nanorods, triangular prisms, disks, and nanoshells) that possess tunable optical properties.[1–4] One common strategy involves the transformation of initially prepared solid spheres into distinct shapes, while other strategies target the direct preparation of shell/core architectures. The optical properties of the resulting nanostructured materials are typically structure-dependent, with the capacity to red- or blue-shift the absorptions and even to generate distinct dipole, quadrupole, and other multipole adsorptions.[5–6] As such, these new nanomaterials are being developed for use in several areas, including imaging, sensing, and various biological applications.[7]

Among several types of metal nanoparticles, those that are based on gold have drawn particular interest due to their biocompatibility, which renders them attractive for use in both *in vitro* and *in vivo* applications.[7] Gold-coated dielectric core particles have received much attention, not only because the resultant materials are expected to be biocompatible, but also because of their tunable optical properties, which can be varied across a wide range of wavelengths from the visible to the near-infrared regions of the spectrum.[8] These particles -- often referred to as "gold nanoshells" -- are typically prepared using a seed-growth method that affords a thin layer of gold around a dielectric silica (SiO_2) core.[9,10] Notably, the diameter of the SiO_2 core and thickness of the gold shell can be specifically controlled during the preparation steps to afford particles with selected absorption wavelengths.[10–11] Importantly, light at wavelengths ranging within the so-called "phototherapeutic window" can penetrate human tissue and water without being absorbed.[12] This window of biological transparency falls squarely between the absorption of common chromophores (<800 nm) and that of water (>1200 nm).[12] A crucial

aspect of photothermal therapy using gold nanoshell (GNS) particles is that the absorption of light leads to rapid and efficient heating of the nanoparticle and therefore the medium surrounding it (*vide infra*).[13]

Our research targets the construction of discrete biocompatible hydrogel-coated GNS particles that undergo structural changes from the heat generated by the GNS core upon exposure to light. Hydrogel polymers are key materials in a variety of technological applications, including catalysis, drug delivery, and chemical separations.[14–16] In aqueous solution, hydrogels undergo abrupt volume transitions that are correlated with the lower critical solution temperature (LCST) and other chemical or physical stimuli, such as pH, ionic strength, and/or solvent composition.[17–20] Hydrogel polymers are typically hydrophilic and well-dispersed in water below the LCST, but become hydrophobic above this temperature.[21-22]

A variety of thermo-sensitive materials that utilize hydrogel-based nanoparticles have been described in the literature; many of these contain poly(N-isopropyl-acrylamide) or "poly(NIPAM)" in either homopolymer or copolymer form.[23–26] Applications involving NIPAM homopolymer hydrogels are somewhat limited because thermally-induced structural changes occur at a fixed LCST of ~30 °C.[27] Researchers have overcome this limitation by incorporating acrylic acid (AAc) or acrylamide (AAm) into the hydrogel polymer matrix, which can shift the LCST of the hydrogel copolymers anywhere from ~30 to 60 °C.[28–29] While AAc or AAm moieties along the poly(NIPAM) backbone serve to increase the LCST, their presence also enhances the large reversible volume changes that poly(NIPAM) undergoes in response to systematic variations in temperature.[28,30-31] Furthermore, these copolymers form relatively thin surface layers that allow soluble materials held inside of the hydrogel particles to be released into the surrounding medium during the collapsing process.[30] It is our belief that these types of hydrogels can be coupled with GNS cores for use as potential drug-delivery carriers or protective containers for biologically active molecules. In addition, the tunable optical properties of the GNS particles will enable these hybrid composite materials to become photothermally-responsive within the aforementioned "phototherapeutic window".

This manuscript describes the use of free radical polymerization[32–34] to coat GNS particless with a thermo-sensitive hydrogel polymer overlayer comprised of NIPAM-co-AAc (Scheme 1). This strategy affords stable and chemically resistant composite nanoparticles that can be used to encapsulate organic and inorganic materials on the nanometer scale. As part of our long-term objective to fabricate light-activated drug-delivery vehicles, this manuscript describes the preparation and characterization of these new hybrid nanoparticles, and demonstrates that the nanomaterials undergo well-behaved structural changes in response to external stimuli (e.g., temperature), providing the platform for a unique nanoscale drug-delivery system that can be optically activated *in vivo*.

Scheme 1. Synthesis of Hydrogel-Coated Gold Nanoshells

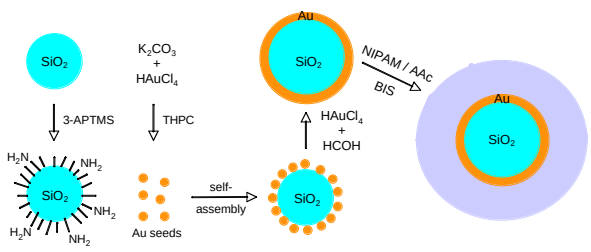

2 EXPERIMENTAL SECTION

2-1. Materials

The following chemicals and reagents were purchased from the indicated suppliers and used as received unless indicated otherwise: formaldehyde (HCOH, 37%), sodium hydroxide (NaOH, 98%), ammonium persulfate (APS, 98%), ammonium hydroxide (30% NH_3), potassium hydroxide (KOH, 85%), nitric acid (HNO_3, 70%), and hydrochloric acid (HCl, 37%), all from EM Science; potassium carbonate (K_2CO_3, 99-100%) and oleic acid (100%), both from J. T. Baker; tetraethylorthosilicate (TEOS, 99%), terakis(hydroxymethyl)phosphonium chloride (THPC, 80% in H_2O), 3-aminopropyltrimethoxysilane (3-APTMS, 97%), all from Aldrich; hydrogen teterachloroaurate(III) hydrate (Strem); and ethanol (McCormick Distilling Co.). N-isopropylacrylamide (NIPAM, 99%) and acrylic acid (AAc, 99.5%) were obtained from Acros; NIPAM was recrystallized in hexane and completely dried under vacuum before use. Water was purified to a resistance of 18 MΩ (Academic Milli-Q Water System; Millipore Corporation) and filtered using a 0.22 μm membrane filter to remove any impurities. All glassware and equipment used in the experiment were first cleaned in an aqua regia solution (3:1, HCl:HNO_3), then cleaned in a base bath (saturated KOH in isopropyl alcohol), and finally rinsed with Milli-Q water prior to use.

2-2. Attachment of Gold Seed Particles to Amine-Functionalized SiO_2 Nanoparticles

Silica nanoparticles with a diameter of ~100 nm were prepared using the conventional Stöber method.[32] Terminal functionalization of the SiO_2 surfaces with amino groups was accomplished using excess 3-APTMS according to the method by Waddell *et al.*[36] The resulting amine-functionalized SiO_2 nanoparticles were then centrifuged using an RC-3B refrigerated centrifuge (Sorvall Instruments) and redispersed in absolute ethanol. No differences between the unfunctionalized and functionalized SiO_2 nanoparticles were detected by field emission scanning electron microscopy (FE-SEM), transmission electron microscopy (TEM), or dynamic light scattering (DLS).

Small gold seed nanoparticles were prepared using the method reported by Duff *et al.*, which utilizes tetrakis(hydroxymethyl)phosphonium chloride (THPC) as the reducing agent.[37–38] In our experiments, the size of THPC-reduced gold seeds could be precisely varied from 2–3 nm in diameter. This solution of gold seeds was aged in the refrigerator for at least three days before use. The aged THPC-reduced gold seeds were then anchored onto the surface of SiO_2 nanoparticles using a modification of the method by Westscott *et al.*[39] This process involved mixing 10 mL of the aged-THPC gold solution (concentrated by a factor ranging from 0.1 to

0.2 after aging) with 1 mL of amine-functionalized SiO_2 nanoparticles overnight. The resultant nanoparticles were then separated by centrifugation and redispersed in 50 mL of Milli-Q water, affording a solution that was light red in color.

2-3. Gold Nanoshell Growth

We used a variation of known methods to grow complete gold shells on the gold-seeded SiO_2 nanoparticle cores.[9,10] First, a basic aqueous gold solution (K-gold solution) was prepared by mixing K_2CO_3 and $HAuCl_4{\cdot}H_2O$ in Milli-Q water. Specifically, 0.025 g of K_2CO_3 was dissolved in 100 mL of Milli-Q water, and then 2 mL of 1 wt% $HAuCl_4{\cdot}H_2O$ was added to the mixture. Within 40 min, the solution changed from yellow to colorless; it was stored in the refrigerator overnight without exposure to light before use. Gold shells were then grown by placing 4 mL of the K-gold solution in a 25 mL beaker equipped with a stir bar, and adding 1.5 mL of the solution of gold-seeded SiO_2 nanoparticles. The mixture was stirred for 10 min, and then 0.02 mL of formaldehyde was added to reduce the K-gold solution. Depending upon the ratio of K-gold solution and gold-seeded SiO_2, the color of the solution changed from colorless to blue (or brown, green), which indicates different thicknesses of gold shells. Adherence to this procedure reliably affords gold nanoshells with absorptions centered at ~850 nm. The gold nanoshells were precipitated by centrifugation and redispersed in Milli-Q water before using as templates for subsequent hydrogel growth.

2-4. Synthesis of Hydrogel-Coated GNS Particles

To avoid aggregation during the polymerization process, the gold nanoshells were washed with 2.5 wt% K_2CO_3 solution. The hydrogel coatings were then grown by polymerization in aqueous solution. The GNS solution was diluted with Milli-Q water to give a maximum absorbance of ~0.4-0.5 a.u. at 850 nm and placed in a three-necked round-bottomed flask equipped with a reflux condenser and an inlet for argon gas. An aliquot of degassed oleic acid (0.0017 mL; 5.4×10^{-6} mol) was then added to the stock solution under argon. The mixture was stirred for 1 h and sonicated for 15 minutes. An approximate 94:6 wt% ratio of NIPAM (0.040 g; 3.5×10^{-4} mol):AAc (0.0024 g; 3.3×10^{-5} mol) and the cross-linker BIS (0.004 g; 2×10^{-5} mol) were added to the mixture and stirred for 15-20 minutes. The mixture was then heated to 70 °C in an oil bath, and the initiator APS (0.005 g; 2.2×10^{-5} mol) was added to promote the polymerization reaction, which was allowed to proceed for 8 h. The solution was cooled to room temperature and filtered through a 1 μm membrane to remove any micron-sized impurities and/or any aggregated particles. The filtered solution was centrifuged twice at 30 °C for 1 h at 3500 rpm, and the supernatant was separated to remove any unreacted materials and soluble side products. The purified hybrid nanoparticles were then diluted with Milli-Q water and stored at room temperature for later characterization. Analysis by DLS showed that the diameter of the hydrogel-coated gold nanoshells could be varied from ~160 nm to ~450 nm through minor variations in the amounts of monomer and initiator as well as the reaction time. We note, however, that the thickest hydrogel coatings were less reproducibly prepared than the thin coatings. We also found examples of multiple GNS cores within a single hydrogel shell in samples having the thickest hydrogel coatings. Thus, we focused the bulk of our characterization efforts on hydrogel-coated gold nanoshells having ~160 nm diameters.

2-5. Characterization Methods

To characterize the GNS particles and the hydrogel-coated GNS particles, we used FE-SEM, energy dispersive X-ray (EDX) analysis, TEM, ultraviolet-visible (UV-vis) spectroscopy, and DLS.

Analysis by FE-SEM was carried out using a JSM 6330F instrument (JEOL) with the ability to perform elemental analysis by EDX (Link ISIS software series 300; Oxford Instruments). To collect the FE-SEM images, gold-seeded SiO_2 nanoparticles, bare gold nanoshells, and hydrogel-coated gold nanoshells were deposited from solution onto Formvar-coated copper grids and completely dried at room temperature overnight prior to analysis. All of the samples were examined with magnification from 30K to 100K to demonstrate the overall uniformity of the nanoparticles.

TEM images were collected using a JEM-2000 FX electron microscope (JEOL) operating at an accelerating voltage of 200 kV. All of the TEM samples were deposited from solution onto 300-mesh Holey carbon-coated copper grids and dried before analysis. Due to the insufficient electron density of the hydrogel polymers, the hydrogel-coated gold nanoshells were mixed with negative staining by 1% uranyl acetate dihydrate to achieve enhanced visualization by TEM.

We employed a Cary 50 Scan UV-vis optical spectrometer (Varian) with Cary Win UV software to characterize the optical properties of the gold-seeded SiO_2 nanoparticles, bare gold nanoshells, and the hydrogel-coated gold nanoshells. UV-vis spectra of the first two types of particles were collected by diluting the samples with Milli-Q water, transferring them to a quartz cell, and scanning over a range of wavelengths (300-1100 nm). The hydrogel-coated gold nanoshells were analyzed as prepared without dilution. For experimental consistency, the spectra of distinct batches of nanoshells were obtained both before and after coating with the hydrogel.

Measurement of the hydrodynamic diameter of the nanoparticles utilized a DLS instrument (ALV-5000 Multiple Tau Digital Correlation) operated at a light source wavelength of 514.5 nm and a fixed scattering angle of 90°. All samples were diluted before analysis. The average hydrodynamic diameter was taken after measuring 5 times for a duration of 100 seconds.

3 RESULTS AND DISCUSSION

Using the procedures described above, gold coatings (~10 nm thick) were successfully grown on gold-seeded SiO_2 cores (~100 nm in diameter), giving shell/core composite nanoparticles with a strong, broad absorption maximum centered at ~850 nm. The resultant gold nanoshells were then used as templates for the growth of

a poly(NIPAM-co-AAc) hydrogel overlayer ranging in thickness from ~20 nm to ~165 nm. Growth of the polymer overlayer was found to be facile and reliable because all of the starting materials were readily soluble; even the GNSs were colloidally well-dispersed in the aqueous medium. This feature circumvented the need for purification steps during the polymerization process. We observed, however, that phase separation sometimes occurred during the reaction, leading to aggregated hydrogel polymers and/or aggregated gold nanoshells if the polymerization conditions (e.g., temperature, amount of initiator and/or monomers) were varied widely. We note that discrete hydrogel-coated gold nanoshell particles are colloidally stable in aqueous solution for several months at room temperature.

Figure 1 shows FE-SEM images of the gold-seeded SiO_2 cores, GNS particles, and hydrogel-coated GNS particles with both thin and thick coatings. The images suggest that there are no significant differences between the gold-seeded SiO_2 cores (Figure 1a) and the bare GNS particles (Figure 1b) in terms of surface morphology, but the diameters of the latter particles are notably larger than those of the former. These figures show further that both the cores and the nanoshells are monodisperse in size. Figure 1c highlights the marked optical contrast of the GNS cores and the hydrogel overlayers. Importantly, the contrast reflects the complete coating of the hydrogel around the GNS particle cores, the former appearing as pale halos around brighter centers. Similarly, Figure 1e and 1f illustrate the growth of substantially thicker hydrogel overlayers on the GNS cores. These images, however, also illustrate a potential drawback of our methodology; namely, the encapsulation of multiple gold nanoshells within a single hydrogel particle matrix. This type of aggregation is rarely observed for the composites having thin hydrogel coatings. Precise control of this particular phenomenon is one of our ongoing research objectives.

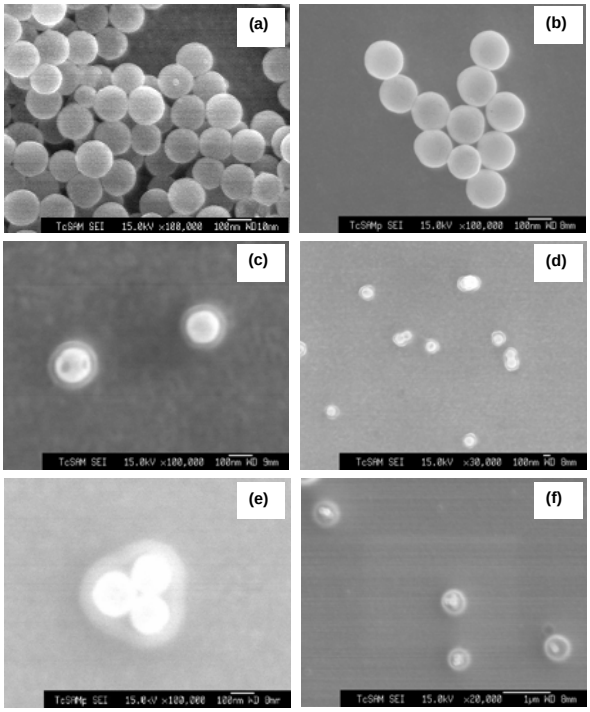

Figure 1. FE-SEM images of (a) gold-seeded SiO_2 cores (~100 nm), (b) bare Au nanoshells (~120 nm), (c) thin hydrogel-coated Au nanoshells (~160 nm), (d) low magnification of (c), (e) thick hydrogel-coated Au nanoshells (~450 nm), (f) low magnification of (e).

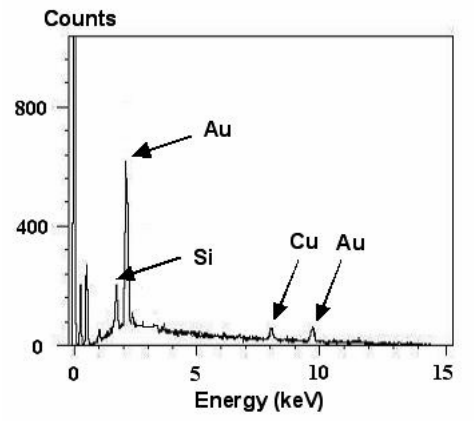

Figure 2. EDX spectrum of hydrogel-coated Au nanoshells (~160 nm in diameter).

In addition to the FE-SEM images, we collected EDX spectra of the hydrogel-coated gold nanoshells to evaluate their elemental composition. Figure 2 presents a representative spectrum showing well-resolved peaks for both gold (Mα and Lα at 2.12 and 9.71 keV) and silica (Kβ and Kβ at 1.75 keV). The observation of silicon in the EDX spectra is due either to the thinness of gold layers (~10 nm), possible defects in the gold shells (e.g., pinholes), and/or the presence of a small number of incomplete gold shells. We observed no peaks that were unambiguously attributable to the hydrogel polymer, which was expected given the low atomic numbers of the constituent elements.

We used TEM to obtain high-resolution images of the hydrogel-coated gold nanoshells (see Figure 3).

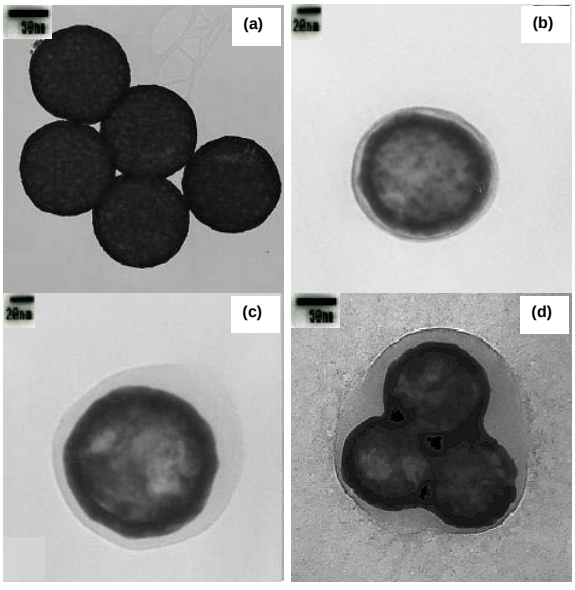

Figure 3. TEM images of (a) bare Au nanoshells (~120 nm), (b) thin hydrogel-coated Au nanoshells (~160 nm), (c) thick hydrogel-coated Au nanoshells, and (d) hydrogel-coated multiple Au nanoshells.

Because of the low electron density of the polymer layer, we selectively stained the AAc groups in the hydrogel polymer backbone with 1% uranyl acetate in water to visualize the hydrogel coating. In Figures 3b and 3c, the hydrogel coating appears as a thin halo surrounding a GNS core particle. We note also that the growth of thick hydrogel coatings on the gold nanoshells often led to a mixture of single and multiple GNS cores within the hydrogel matrix (see Figure 3c and 3d), which is consistent with the observations by FE-SEM (Figures 1e and 1f). Taken as a whole, these images provide unequivocal evidence that the hydrogel coatings surround the GNS cores. We note, however, that much smaller hydrogel diameters were observed by TEM compared to those observed by FE-SEM (*vide supra*) and DLS (*vide infra*), perhaps due to the high vacuum and strong electron beam used in the collection of the TEM data.

Figure 4 shows the UV-vis absorption spectra of the gold-seeded SiO_2 cores, bare gold nanoshells, and hydrogel-coated gold nanoshells. For the gold-seeded cores, the absorption maximum appears at 520-530 nm, which is characteristic of unaggregated small gold nanoparticles; in contrast, the absorption maxima of gold nanoshells range typically from 700 to 950 nm, and the bands are characteristically broad.[9] Studies have shown that the intensity and broadness of gold nanoshell absorption bands depend on the completeness and morphology of the gold coating on the SiO_2 cores.[40] Given the position, intensity, and broadness of the absorption bands centered at ~850 nm in Figure 4, we conclude that complete gold overlayers were grown on the SiO_2 cores utilized here.[9] Furthermore, due to the thinness of the hydrogel coating, the band position and intensity observed for the hydrogel-coated gold nanoshells are similar to those observed for the bare nanoshells (i.e., the hydrogel coating exerts no strong influence on the adsorption maximum). We note, however, a slight increase in band intensity at 300–600 nm for the hydrogel-coated particles; this increase is probably due to scattering from the hydrogel matrix.

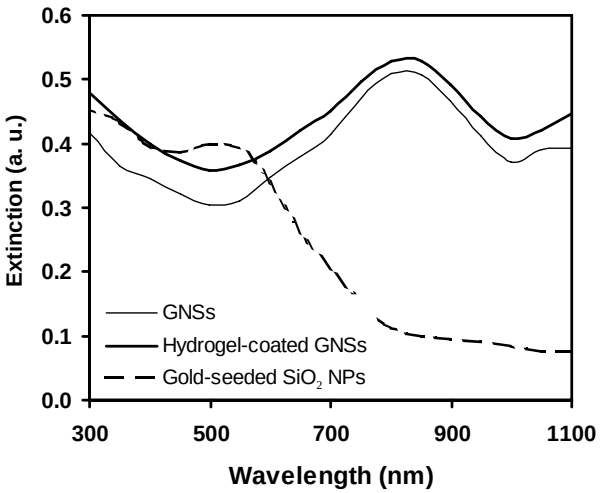

Figure 4. UV-vis spectra of gold-seeded SiO_2 cores, bare Au nanoshells, and hydrogel-coated Au nanoshells.

At dilute neutral pH, we used DLS to monitor systematic changes in the hydrodynamic diameter of the hydrogel-coated gold nanoshells as a function of alternating temperature; under these same conditions, the hydrodynamic diameter of bare gold nanoshells was invariant (see Figure 5). Specifically, the diameters of the bare nanoshells (~120 nm) remained constant as the temperature was switched between 25 °C and 45 °C; in contrast, the diameters of the hydrogel-coated nanoshells decreased by ~30 nm upon heating to 45 °C, but swelled to their original size upon cooling to 25 °C. The cooling and heating process was repeated several times, and the hydrogel-coated particles showed similar reversibility every time, providing indirect support for the presence of a NIPAM-based hydrogel coating on the gold nanoshell cores.[41–43]

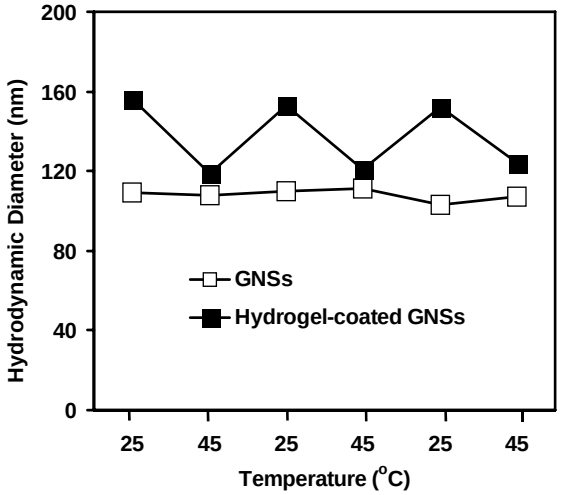

Figure 5. The hydrodynamic diameters of bare Au nanoshells and hydrogel-coated Au nanoshells as a function of alternating temperature.

The collapse of the hydrogel polymers above the LCST arises from a loss of hydrogen bonding between water and hydrophilic sites along the hydrogel polymer backbone, such as amide groups for poly(NIPAM).[31,41] Above the LCST, it has been proposed that the loss of hydrogen bonding between water and the polymer backbone removes internal electrostatic repulsion within the hydrogel polymer matrix, leading to a collapse of the hydrogel structure.[41] The controlled incorporation of ionizable groups, such as AAc, into the backbone can be used to fine tune the negative electrostatic environment. The presence of additional strongly hydrophilic moieties not only enhances the water-swelling properties, but also increases the LCST.[42] For example, the LCST of pure poly(NIPAM) hydrogels is fixed at ~30 °C, but that of poly(NIPAM-co-AAc) hydrogels containing 5% AAc moieties is known to be higher, ranging from 34 to 40 °C.[41,43] It is important to note that access to the upper part of this temperature range renders these polymers attractive for use as dynamic materials in the human body, where the ambient temperature is 37 °C.

We recently described the synthesis and study of poly(NIPAM)-coated nanoparticles in which the core consisted of a simple gold nanoparticle rather than a gold nanoshell.[44] In the course of the investigation, we found that the incorporation of 5% AAc moieties led to a

small increase in the LCST compared to that reported for free-standing poly(NIPAM-co-AAc) hydrogels.[41,43] This modest increase probably arises from a reduction in the average interchain distance in hydrogel polymers that is cause by anchoring to surface of the metal nanoparticles.[44] Despite this noted difference, it should still be possible to tune the LCST above physiological temperature simply by increasing the content of the AAc moieties in the co-polymer matrix.[31,41,43]

As noted in the Introduction, light at wavelengths ranging from 800–1200 nm can penetrate human skin and bone without harming the tissue.[45] As such, the hydrogel-coated GNS particles described here represent a unique thermo-responsive system that can be activated *in vivo*. Furthermore, impregnation of the hydrogel coatings with therapeutic agents (e.g., pharmaceuticals such as insulin or cisplatin) offer the possibility of targeted drug delivery that can be controlled optically.[46] Studies of drug loading and delivery using these nanoparticles are currently being conducted.

4 CONCLUSIONS

Thin gold shells were reliably grown on SiO_2 nanoparticle cores, and the encapsulation of these particles within a thermo-responsive hydrogel polymer overlayer having tunable thickness was demonstrated. Gold nanoshells with diameters of ~120 nm displayed strong optical absorptions centered at ~850 nm. The resulting individual nanoshells were then coated with a poly(NIPAM-co-AAc) hydrogel polymer having thicknesses ranging from ~20 nm to ~160 nm. We found that the growth of thin coatings on individual cores particles was facile and reproducible; in contrast, efforts to grow thick coatings sometimes led to the encapsulation of multiple cores along with single cores. The morphology, elemental composition, and optical properties of these composite nanoparticles were fully characterized by FE-SEM, EDX, TEM, and UV-vis spectroscopy. These data collectively demonstrate the formation of discrete hydrogel-coated gold nanoshells. Analysis by DLS showed that the hydrodynamic diameters of the hydrogel-coated particles decrease with an increase in temperature from 25 to 40 °C, but then reversibly swell to their original size upon cooling back to 25 °C. As a whole, the composition and physical characteristics of these unique nanomaterials appear to be ideally suited for their intended use nanoscale drug-delivery vehicles.

ACKNOWLEDGMENTS

We thank the Army Research Office, the National Science Foundation (ECS-0404308), the Texas Center for Superconductivity, and the Robert A. Welch Foundation (Grant E-1320) for their generous financial support of this work. We also thank Dr. I. Rusakova for assistance with the TEM measurements and Dr. J. C. Reina for assistance with the DLS measurements. Use of the DLS instrument was made possible by a grant from the Department of Energy to Professor Simon Moss (UH).

REFERENCES

[1] Sun, Y.; Mayers, B.; Xia, Y. *Nano Lett.* **2003**, *3*, 675.

[2] Kim, F.; Song, J. H.; Yang, P. *J. Am. Chem. Soc.* **2002**, *124*, 14316.

[3] Graf, C.; Blaaderen, A. V. *Langmuir* **2002**, *18*, 524.

[4] Hao, E.; Kelly, K. L.; Hupp, J. T.; Schatz, G. C. *J. Am. Chem. Soc.* **2002**, *124*, 15182.

[5] Kelly, K. L.; Coronado, E.; Zhao, L. L; Schatz, G. C. *J. Phys. Chem. B* **2003**, *107*, 668.

[6] Link, S.; El-Sayed, M. A. *J. Phys. Chem. B* **1999**, *103*, 8410.

[7] Cao, Y.–W.; Jin, R.; Mirkin, C. A. *J. Am. Chem. Soc.* **2001**, *123*, 7961.

[8] Oldenburg, S. J.; Jackson, J. B.; Westcott, S. L.; Halas, N. J. *Appl. Phys. Lett.* **1999**, *75*, 2897.

[9] Oldenburg, S. J.; Averitt, R. D.; Westcott, S. L.; Halas, N. J. *Chem. Phys. Lett.* **1998**, *288*, 243.

[10] Pham, T.; Jackson, J. B.; Halas, N. J.; Lee, T. R. *Langmuir* **2002**, *18*, 4915.

[11] Averitt, R. D.; Westcott, S. L.; Halas, N. J. *J. Opt. Soc. Am. B* **1999**, *16*, 1824.

[12] Simpson, C. R.; Kohl, M.; Essenpreis, M.; Cope, M. *Phys. Med. Biol.* **1998**, *43*, 2465.

[13] Gorelikov, I.; Field, L. M.; Kumacheva, E. *J. Am. Chem. Soc.* **2004**, *126*, 15938.

[14] Pelton, R. *Adv. Coll. Interface Sci.* **2000**, *85*, 1.

[15] Bergbreiter, D. E.; Case, B. L.; Liu, Y. S.; Caraway, J. W. *Macromolecules* **1998**, *31*, 6053.

[16] Jeong, B.; Bae, Y. H.; Lee, D. S.; Kim, S. W. *Nature* **1997**, *388*, 860.

[17] Lokuge, I.; Wang, X., Bohn, P. W. *Langmuir* **2007**, *23*, 305.

[18] Schild, H. G.; Tirrell, D. A. *J. Phys. Chem.* **1990**, *94*, 4352.

[19] Saunders, B. R.; Vincent, B. *J. Chem. Soc. Faraday Trans.* **1996**, *92*, 3385.

[20] Zhou, S.; Chu, B. *J. Phys. Chem. B* **1998**, *102*, 1364.

[21] Winnik, F. M. *Polymer* **1990**, *31*, 2125.

[22] Ionov, L.; Stamm, M.; Diez, S. *Nano Lett.* **2006**, *6*, 1982.

[23] Gao, H.; Yang, W. Y.; Min, K.; Zha, L,; Wang, C. *Polymer* **2005**, *46*, 1087.

[24] Snowden, M. J.; Tomas, D.; Vincent, B. *Analyst* **1993**, *118*, 1367.

[25] Jones, C. D.; Lyon, L. A. *Macromolecules* **2003**, *36*, 1988.

[26] Zhu, M.–Q.; Wang, L.-Q.; Exarhos, G. J.; Li, A. D. Q. *J. Am. Chem. Soc.* **2004**, *126*, 2656.

[27] Pelton, R. H.; Pelton, H. M.; Morphesis, A.; Rowell, R. L. *Langmuir* **1989**, *5*, 816.

[28] Snowden, M. J.; Chowdhry, B. Z.; Vincent, B.; Morris, G. E.; *J. Chem. Soc. Faraday Trans.* **1996**, *92*, 5013.

[29] Priest, J. H.; Murray, S. L.; Nelson, R. J.; Hoffman, A. S. *Reversible Polym. Gels. Rel. Syst.* **1987**, *350*, 255.

[30] Yoshida, R.; Sakai, K.; Okano, T.; Sakuri, Y. *J. Biomater. Sci., Polym. Edn.* **1994**, *6*, 585.

[31] Pagonis, K.; Bokias, G. *Poly. Bull.* **2007**, *58*, 289.

[32] Saunders, B. R.; Vincent, B. *Adv. Coll. Interface Sci.* **1999**, *80*, 1.

[33] Saunders, B. R.; Crowther, H. M.; Vincent, B. *Macromolecules* **1997**, *30*, 482.

[34] Neyret, S.; Vincent, B. *Polymer* **1997**, *38*, 6129.

[35] Stöber, W.; Fink, A.; Bohn, E. *J. Colloid Interface Sci.* **1968**, *26*, 62.

[36] Waddell, T. G.; Leyden, D. E.; DeBello, M. T. *J. Am. Chem. Soc.* **1981**, *103*, 5303.

[37] Duff, D. G.; Baiker, A.; Edwards, P. P. *Langmuir* **1993**, *9*, 2301.

[38] Duff, D. G.; Baiker, A.; Gameson, I.; Edwards, P. P. *Langmuir* **1993**, *9*, 2310.

[39] Westscott, S. L.; Oldenburg, S. J.; Lee, T. R.; Halas, N. J. *Langmuir* **1998**, *14*, 5396.

[40] Charnay, C.; Lee, A.; Man, S.; Moran, C. E.; Radloff, C.; Bradley, R. K.; Halas, N. J. *J. Phys. Chem. B* **2003**, *107*, 7327.

[41] Shibayama, M.; Mizutani, S.; Nomura, S. *Macromolecules* **1996**, *29*, 2019.

[42] Kato, E. *J. Chem. Phys.* **1997**, *106*, 3792.

[43] Tan, K. C.; Wu, X. Y.; Pelton, R. H. *Polymer* **1992**, *33*, 436.

[44] Kim, J.–H.; Lee, T. R. *Chem. Mater.* **2004**, *15*, 4169.

[45] Sershen, S. R.; Westcott, S. L.; Halas, N. J.; West, J. L. *J. Biomed. Mater. Res.* **2000**, *51*, 293.

[46] Kim, J.–H.; Lee, T. R. *Drug Dev. Res.* **2006**, *67*, 61.

